中国激光

超快激光在无源光波导器件制造中的应用综述

丁烨，李强*，李靖怡，王联甫，杨立军**

哈尔滨工业大学机电工程学院，黑龙江 哈尔滨 150001

摘要 我国航空、航天等领域的发展推动着全光通信、光信息处理等技术的不断革新。光波导器件作为关键一环，其制备工艺对性能的影响至关重要。超快激光作为一种新型的激光光源，具有极高的能量密度和极短的脉宽，这些特性使得超快激光加工后几乎无热影响区、重铸层等缺陷残留。将超快激光用于制备光波导器件已成为工业界研究的热门领域之一。本文首先阐述了超快激光与常用波导材料的微观作用机理。针对国内外学者利用超快激光制备无源光波导器件的相关研究进行系统综述，详细阐述了光路变换器、功率分配器和波导型透镜等典型无源光波导器件的超快激光制备方法和器件性能；结合当前研究进展和面临的主要问题的分析，对未来超快激光制备无源光波导器件技术的发展方向进行展望。

关键词 激光技术；超快激光；无源光波导器件；制备工艺；器件性能

中图分类号 TN249；TN252 **文献标志码** A **doi**：10.3788/CJL202148.0802020

1 引 言

随着我国航空、航天、通信、仪表等领域的不断发展，传统的光学、电学系统已经难以满足大容量、高速率的信息传输需求[1]。集成光学就是在这种历史条件下逐渐发展起来的，其特点是将不同功能的分立光学器件集成在一个很小的区域内，对光信号进行低功耗和高稳定性的高速传输和处理[2]。相比于传统的光学系统，集成光学系统具有体积小、结构紧凑、稳定性高、抗干扰能力强等优势。光波导器件是集成光学系统的基本单位，其原理在于利用光在不同折射率的介质中传播时在介质界面上发生全反射，从而将光限制在微米级尺度的结构内，形成引导光波沿着一定方向传播的导光通道。光波导器件不仅可以限制和引导光的传输，还具有非线性、主动增益等功能[3]；同时，与集成光路中的其他元件结合，可以形成拥有多种功能的高密度集成光子芯片，实现复杂化、微型化、多样化的应用[4-5]。光波导器件性能的优劣直接影响了集成光路的整体性能。开发光波导器件的高质量、高精度制备工艺技术，对于提升集成光路性能，推动光通信、光信息处理、光计算及光传感等技术的革新以及国家重点领域高端装备的发展具有重要意义。

光波导器件可分为不受外场控制的无源器件和受外场控制的有源器件，而前者是集成光电子学的基础，应用更为广泛[6]。构成无源光波导器件的材料主要有半导体、有机聚合物等。半导体光波导可分为硅基波导、Ⅲ-Ⅳ族化合物材料波导以及铁电氧化物材料波导。其中硅基光波导的优势表现为良好的热传导性和化学稳定性、优异的机械强度、低吸收损耗，缺点则是包层和芯层的折射率差异较大；Ⅲ-Ⅳ族化合物材料波导的优势在于可以和有源器件集成在同一芯片上，但是其传输损耗大，物料成本高；铁电氧化物材料波导具有较大的电光系数、较快的响应速度、优异的热稳定性和化学稳定性，但其缺点在于物料成本高，形成的器件尺寸较大。聚合物光波导具有较低的光损耗和双折射率、较高的热光系数和电光系数、制作工艺简单等优势，但是易于老化，不利于提高器件的稳定性。

制备光波导器件的方法可分为脱膜法、腐蚀法

收稿日期：2020-11-30；**修回日期**：2021-01-03；**录用日期**：2021-02-25

基金项目：国家重点研发计划(2017YFB1104900)、中国博士后科学基金(2020M670900)、黑龙江省博士后面上资助(LBH-Z20054)

* **E-mail**：1577014781@qq.com；** **E-mail**：yljtj@hit.edu.cn

和直写法三类。脱膜法是在衬底表面涂胶形成光刻图并利用有机溶剂溶解抗蚀剂形成光波导[7]，可实现亚微米尺度结构的精细加工，但不适用于在薄膜沉积过程中存在高温工艺的工况。腐蚀法可分为化学湿法刻蚀和离子束溅射刻蚀等，需要在光波导层表面上制作出掩模层图形，通过对掩模开窗口部位进行腐蚀加工形成光波导[8]。该方法的设备成本较低，不会对样品造成额外损伤，但可重复性较低，且是各向同性腐蚀，加工精度难以达到亚微米量级。直写法主要是利用具有极高峰值功率密度和极短脉宽的超快激光改变写入区域材料的微观结构形貌与光学、力学等性能，形成光波导。相比于上述技术，超快激光直写技术具有突破衍射极限的加工尺度，高度柔性的加工策略，较强的材料适应性，可精准控制作用过程，无需掩模或其他预、后处理技术等优势[9]。1996 年，Davis 等[10]率先利用超快激光在光学玻璃内制备了光波导。此后，随着超快激光设备升级以及加工工艺的改进，国内外学者在诸多材料内成功制备了光波导，并且实现了光波导器件的多种应用。

本文主要针对无源光波导器件的超快激光制备工艺进行较为完备的综述。首先，分析了超快激光与半导体和电介质等光波导器件材料的微观作用机理；然后，系统地列举了国内外学者利用超快激光技术制备光路变换器、功率分配器、波导型透镜等典型无源光波导器件的方法及其工作性能；最后，对当前的研究进展和面临的主要问题进行了分析，并对超快激光在制备无源光波导器件中的应用趋势进行了展望。

2　超快激光与波导材料的作用机理分析

超快激光与波导材料的作用机理取决于材料微观电子系统的特性，大致可分为两类。

1）半导体。超快激光与半导体材料的作用机制取决于其带隙能量和光子能量的相对大小。若材料的带隙能量低于激光单光子能量，则其激光辐照过程中表现出类金属特性；若材料的带隙能量高于激光单光子能量，则其对激光能量的吸收过程与电介质类似。此外，超快激光辐照半导体过程中还会发生“非热性”结构转变[11]，即电子吸收激光能量后逐渐形成等离子体，此时晶格仍保持低温状态。大约 10%的价带电子脱离价带后，晶格结构发生弱化，导致原子的流动性增强，材料内部发生结构性转换，形成不定形态结构。

2）电介质。电介质材料内部无自由电子和离子，典型代表有聚合物等。超快激光辐照时的能量耦合过程在时间尺度上可分为如下步骤：

步骤 1　通过多光子电离或隧道电离在电介质内产生自由电子和载流子。通过非线性效应激发产生的电子还会经过声子调制的线性激光吸收直接获得能量来激发其他的价带电子，即雪崩电离。经过多种机制产生的自由电子密度达到一定阈值时，自由电子就会展现出一定的共振等离子体特性，具体表现为对后续激光能量的高反射和高吸收[12]。

步骤 2　沉积在自由电子上的能量向晶格系统扩散。这一过程只受外部环境干扰，超快激光并不直接参与。在约 1 ps 的时间量级上，部分被电子吸收的能量逐渐向晶格转移。在纳秒量级上，致密等离子体向周围扩散，在辐照区域形成冲击波。在毫秒量级上，辐照区域累积的激光能量以热扩散的形式向未辐照区域扩散，引起局部材料改性等[13]。

超快激光辐照后，电介质材料吸收的能量通过两种方式不断释放，即热消耗和形成冲击波后再作用于周围材料的方式。通过这两种方式，晶格接收到能量，导致后续的折射率改变，这一过程可通过热效应模型[14]、色心模型[15]、材料结构改变稠密化模型[16]等综合解释。但这些模型均指出，当单位面积辐照的激光能量密度过高时，会引起较为显著的热损伤。这会极大地降低光波导结构的完整性，引起折射率的不均匀分布，不利于光信号在波导结构内传输，进而削弱了光波导器件的工作性能。当单位面积上辐照的激光能量密度被控制在合理的范围内时，加工区域更为光整，应力分布与折射率改变也更为均匀，有利于制备高性能的光波导器件。此外，超快激光脉冲的时间和空间分布对于电介质的结构与折射率改变也具有不可忽视的影响。

3　光路变换器的超快激光制备

集成光路一般可分为混合集成光路和单片集成光路。混合集成光路是将两种以上的衬底材料结合在一起，使得不同器件的光特性最优化；而单片集成光路则是在单个衬底材料上集成多个器件。相比于前者，后者更有利于提升光学器件的整体集成度。若要实现单个衬底上多个光学器件的互连耦合，则需要制备光路变换器，改变光路方向，其中以弯曲光波导最为常见。

Sun 等[17]利用数值孔径（NA）为 0.46 的物镜

将脉冲能量为 7.1 μJ 的超快激光聚焦至硼硅酸盐玻璃内，在三维精密位移台和后续超声乙醇浴的配合下制备出半径为 5 mm、弧度为 90°的光波导，如图 1(a)所示。通过可见光耦合对波导性能进行测试，结果表明大多数散射发生在波导边界，而波导中心的散射较少，整体损耗为 3～5 dB/cm @ 632.8 nm。Dreisow 等[18]采用相似的实验设备，在熔融石英中制备了正弦型弯曲波导，并通过分析色心的荧光对比了具有不同周期、峰值高度的波导工作时的损耗程度，如图 1(b)所示。Arriola 等[19]利用 *NA* 为 1.25 的油镜将脉冲能量为 90 nJ 的超快激光聚焦至硼铝硅酸盐玻璃内，制备出曲率半径不同的圆角弯曲波导，并通过速率退火工艺，首先将工件加热至相变温度以上，再采用极低的冷却速率使工件温度缓慢降低至应变点，消除超快激光辐照引起的局部压力和双折射效应。退火后波导核心的折射率降低至 8.4×10^{-3}，耦合损耗降低至 0.25 dB/cm @ 1550 nm，退火后的波导形貌及退火前后折射率对比如图 1(c)所示。Lü 等[20]采用柱透镜组和狭缝对超快激光束进行整形，这一方法尽管造成了一定的能量损失，但制备的 L 型直角波导截面从椭圆形改进为圆形，传输损耗仅为 0.6 dB/cm@976 nm，如图 1(d)所示。通过数值仿真建立了波导输入输出段相交区域长度与弯曲效率的关联，结果表明，当相交区域的长度在合理范围内，波导的弯曲效率可达 81.6%。He 等[21-22]在超快激光直写光路中增加一对距离为 180 mm、空间周期为 1200 lp/mm 的平行光栅，用以分离入射激光束 *X* 方向的光谱分量以及

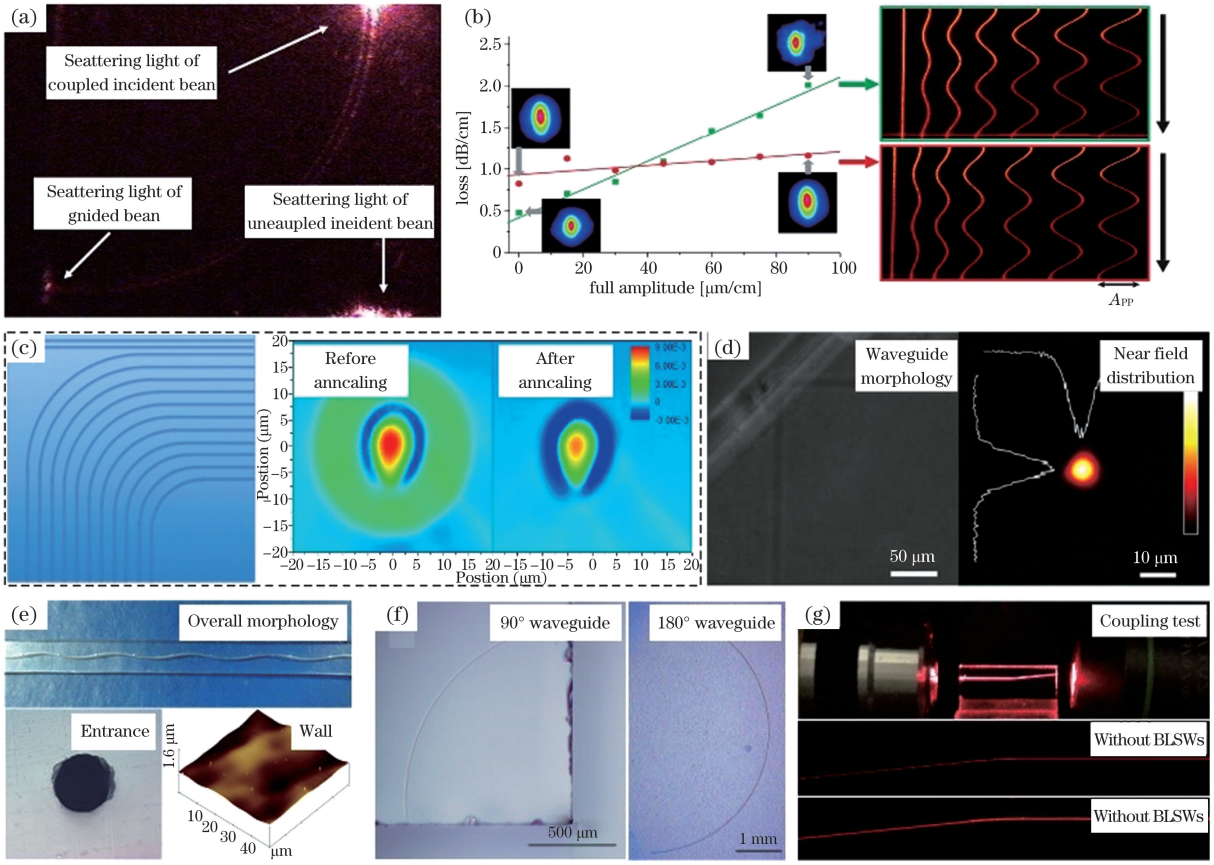

图 1　超快激光制备光路变换器的部分研究成果。(a) 90°波导的导光过程[17]；(b)周期及幅值不同的正弦形波导形貌及其导光损耗[18]；(c)圆角矩形波导形貌以及退火前后截面折射率分布[19]；(d)直角波导以及导引光的近场分布[20]；(e)波浪形波导及其局部形貌[21-22]；(f) 90°波导和半圆形波导[23]；(g)直写光路中有无弯曲损耗抑制面对导光损耗的影响[24]

Fig. 1　Several achievements of ultrafast laser manufacturing of optical path converters. (a) Waveguide illumination using 90°-shaped waveguide[17]; (b) sinusoidal-curve-shaped waveguide with different periods and amplitudes and their guiding losses[18]; (c) rounded-rectangle-shaped waveguides and the distribution of refractive index of their cross-section before and after annealing[19]; (d) right-angle-shaped waveguide and the near-field distribution of guiding beam[20]; (e) wave-like waveguide and its local morphology[21-22]; (f) 90°-shaped and half-ring-shaped waveguides[23]; (g) influence of BLSWs on guiding losses[24]

调控焦点处的能量密度分布。同时，采用三步式制备工艺，即首先用超快激光在熔融石英内制备光波导，再将工件浸泡在 KOH 溶液中进行超声浴，对激光辐照区域进行选择性蚀除，最后将工件放置在熔炉中进行退火，对波导结构内壁进行光整化处理。制备的波浪型光波导形貌如图 1(e)所示。退火后波导内壁粗糙度 R_a 降低至 4.6 nm，光束传输效率提升至 90%，接近理论极限值。Suzuki 等[23]则在直写光路中增加 C 型玻璃全息图(经电子光刻和反应离子刻蚀形成)，将激光束转变为半圆形分布，在无需工作台的前提下直接在熔融石英中制出曲率半径和弧度各异的光波导，如图 1(f)所示。Liu 等[24]采用圆形偏振激光来避免线偏振诱导产生的周期性纳米结构对波导性能的影响，并且在物镜的光瞳面增加了自适应狭缝结构。在制备弯曲光波导的过程中，激光扫描方向保持不变，而狭缝的方向不断改变，保证其与工件移动方向一致，从而有效避免了方向弯曲效应。为进一步降低波导的弯曲损耗，在单根波导的两侧制备了弯曲损耗抑制面(BLSWs)，形成“三明治”结构。通过调整该面的结构，曲率半径为 15 mm 的光波导损耗降低了约 90%@633 nm，如图 1(g)所示。

4　功率分配器的超快激光制备

功率分配器是将入射光的功率按照预定的比例分成两束及以上输出激光的光波导器件，它是光通信系统中将信号从干线光缆分配到各用户时必不可少的器件。功率分配器主要有分支光波导和方向耦合器两大类。

4.1　分支光波导

分支光波导的前部有一个喇叭状波导，目的是防止在分支点处产生额外的横模。考虑到散射损耗和性能稳定性，分支光波导的分叉角、分叉长度和局部质量都有一定的限制。Lü 等[25]采用 *NA* 为 0.6 的物镜将脉冲能量为 4.9 μJ 的超快激光束聚焦至铌酸锂晶体中，结合 *Z* 切的方式在铌酸锂晶体内制出对称二分支型(1×2)和四分支型(1×4)波导分束器，每两个分支波导的夹角约为 0.229°，长度约为 32 μm。当输入激光为基模时，1×2 分束器在 632.8 nm 和 1064 nm 波段的输出能量比均为 50∶50，1×4 分束器在 632.8 nm 和 1064 nm 波段的输出能量比为 50∶48∶50∶49 和 50∶48∶49∶48，二者均展现出良好的分光性能，如图 2(a)所示。He 等[26]采用相似的直写方法和 0.14 μJ 的脉冲能量，在锗酸铋($Bi_4Ge_3O_{12}$)晶体内制出对称二分支、三分支和四分支型波导分束器，每两个输出分支波导的夹角约为 0.4°，分支波导内最大折射率变化为 $(5.3\pm1)\times10^{-3}$。近场耦合测试结果表明，分支波导在 TE 和 TM 偏振下均能保持良好的基模传递，传输损耗低于 4 dB/cm@4 μm，如图 2(b)所示。Ren 等[27]利用 *NA* 为 0.4 的物镜将线偏振超快激光聚焦至钛蓝宝石晶体内部，通过控制三维平台，使得工件沿垂直于光束传播的方向以 500 μm/s 速度移动，在晶体内制出输出通道端面尺寸、中心距离和夹角不同的嵌入包层式对称二分支型波导分束器，如图 2(c)所示。这些分束器在 TE 和 TM 偏振下对可见和近红外光束进行有效限制，保持了良好的荧光特性。Cheng 等[28]采用同样的实验设备，在钽酸锂($LiTaO_3$)晶体中制出与上述结构和性能类似的波导分束器。Mittholiya 等[29]采用 200 kHz 的高重复频率和 4 μm/s 的低直写速度，在硼硅酸盐玻璃内制备对称二分支、四分支和八分支型波导分束器，如图 2(d)所示。相比于在低重复频率、高直写速度、多扫描次数条件下制备的光波导，该方法制备的波导结构虽然耦合损耗和传输损耗略有增加，但分束后能量分布更为均匀。Chen 等[30]首先用通量为 4×10^{14} ion/cm^2 的 O^{5+} 离子束以 7°的倾斜角注入砷酸钛氧钾($KTiOAsO_4$)晶体，对晶体表层的折射率进行修改；然后采用超快激光在改性层和基体内刻蚀出分叉角分别为 1.5°和 2°的对称二分支型波导分束器，分支部分壁面粗糙度约为 1 μm。测试结果表明，两种分束器在 633 nm 和 808 nm 工作时其传输损耗与入射耦合激光的偏振方向有显著关联，即当入射激光沿着 TE 方向偏振时，传输损耗最低，而沿着 TM 方向偏振时，传输损耗最高，如图 2(e)所示。Tao 等[31]为提升光电印刷电路板的性能，在基底石英玻璃表面旋涂一层 SU8 聚合物，以空气为波导镀层，利用超快激光在聚合物层中直写出对称十六分支型波导分束器。通过控制旋涂速度、激光脉冲能量和直写速度，实现波导尺寸、壁面粗糙度以及波导性能的调控。波导性能的测试仿真与实验结果与 Chen 等[30]和 Landowski 等[32]的结果类似，即当入射激光沿着 0°和 180°偏振时，传输损耗最低，沿着 90°和 270°偏振时，传输损耗最高，如图 2(f)所示。

4.2　方向耦合器

与分支光波导不同的是，方向耦合器的分支之间并无交叉，而是存在间隙为微米量级的平行耦合

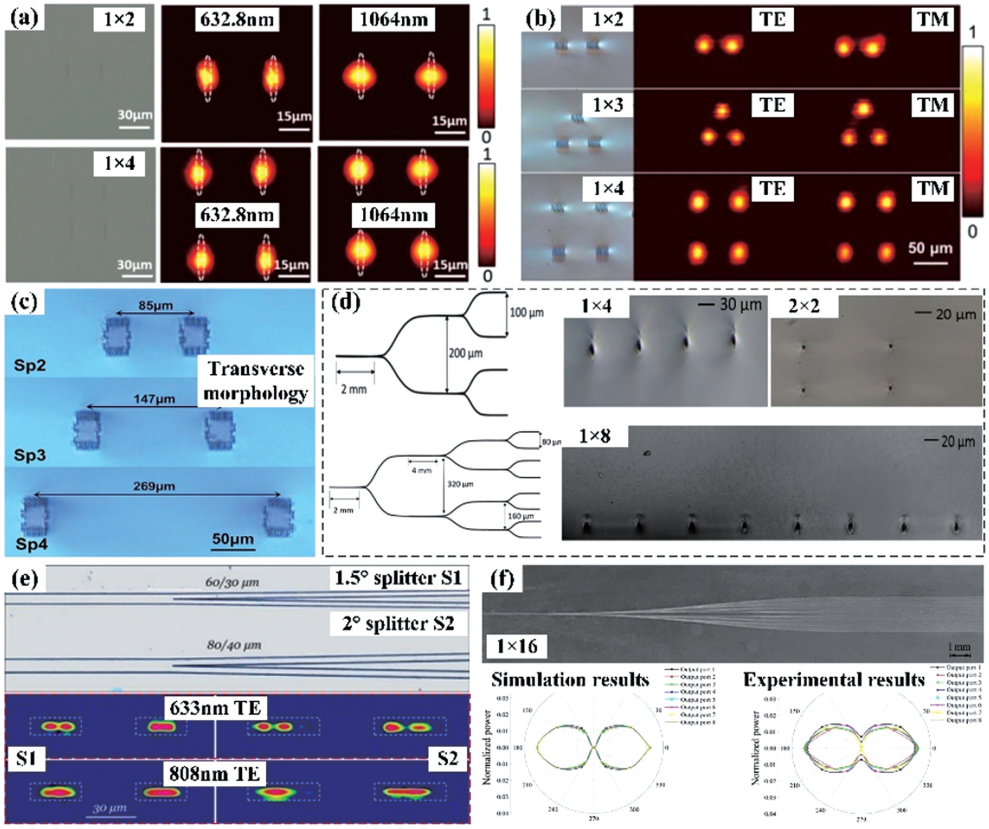

图 2　超快激光制备分支光波导的部分研究成果。(a)对称二分支和四分支型分束器及其在不同波段下的分光性能[25]；(b)对称二分支、三分支和四分支型分束器及其在不同偏振状态下的分光性能[26]；(c)嵌入包层式对称二分支型分束器端面形貌[27]；(d)对称四分支和八分支型分束器端面形貌[29]；(e)分叉角不同的分束器以及不同波段下的分光性能[30]；(f)对称十六分支分束器以及仿真和实验获得的不同偏振状态下的分光性能[31]

Fig. 2 Several achievements of ultrafast laser manufacturing of branched waveguides. (a) Symmetric 1×2 and 1×4 splitters and their performance under different wavelengths[25]; (b) symmetric 1×2, 1×3, and 1×4 splitters and their performance under different polarizations[26]; (c) transverse plane morphology of embedded cladding symmetric 1×2 splitter[27]; (d) transverse plane morphologies of symmetric 1×4 and 1×8 splitters[29]; (e) splitters with different branch angles and their performance under different wavelengths[30]; (f) symmetric 1×16 splitter and its performance under different polarizations obtained by simulations and experiments[31]

段。2006 年，Sowa 等[33]率先在甲基丙烯酸甲酯(PMMA)中实现了方向耦合器的超快激光直写。在直写过程中，为调整激光的偏振状态，防止在工件内诱导产生不规则空腔，在光路中添加了狭缝，并将脉冲能量设置为 27 nJ。通过调整耦合段的长度，实现分光比例的调控，如图 3(a)所示。Chen 等[34]在铝硅酸盐玻璃中直写出可在宽波段(1250～1650 nm)下工作的方向耦合器，弯曲段的曲率半径为 50 mm，耦合段长度为 0～2.5 mm，耦合段间隙为 6～10 μm，其中耦合器一侧直写速度保持 12 mm/s，另一侧直写速度为 8～20 mm/s。当两侧直写速度一致时，可通过补偿弯曲段和耦合段之间的波长离散度来提升耦合效率；当两侧直写速度不一致时，可通过抑制弯曲段的波长离散度来提升耦合效率(从 2% 提升至 87%)，如图 3(b)所示。Zhang 等[35]为避免光路引起的球差对直写区域材料折射率和波导耦合效率的影响，采用 *NA* 高达 1.4 的物镜和荧光浸油法聚焦激光束，并使用空间光调制器和相位掩模法将激光束的截面调整为纵向环形分布，在掺 MgO 的铌酸锂晶体中直写出可重构的对称双向耦合器。当输入激光为 H 线偏振光和 V 线偏振光时，该耦合器均表现出良好的耦合性能。Skryabin 等[36]在物镜前增加焦距分别为 200 mm 和 60 mm 的柱透镜组合，将聚焦后的激光束腰直径增加约 3.3 倍，瑞利长度降低约 70%，在钇铝石榴石晶体内制出对称二向二分支、对称二分支和对称三向三分支型方向耦合器，并且在量子存储单元中得到应用，如图3(c)所示，其中，每个方向

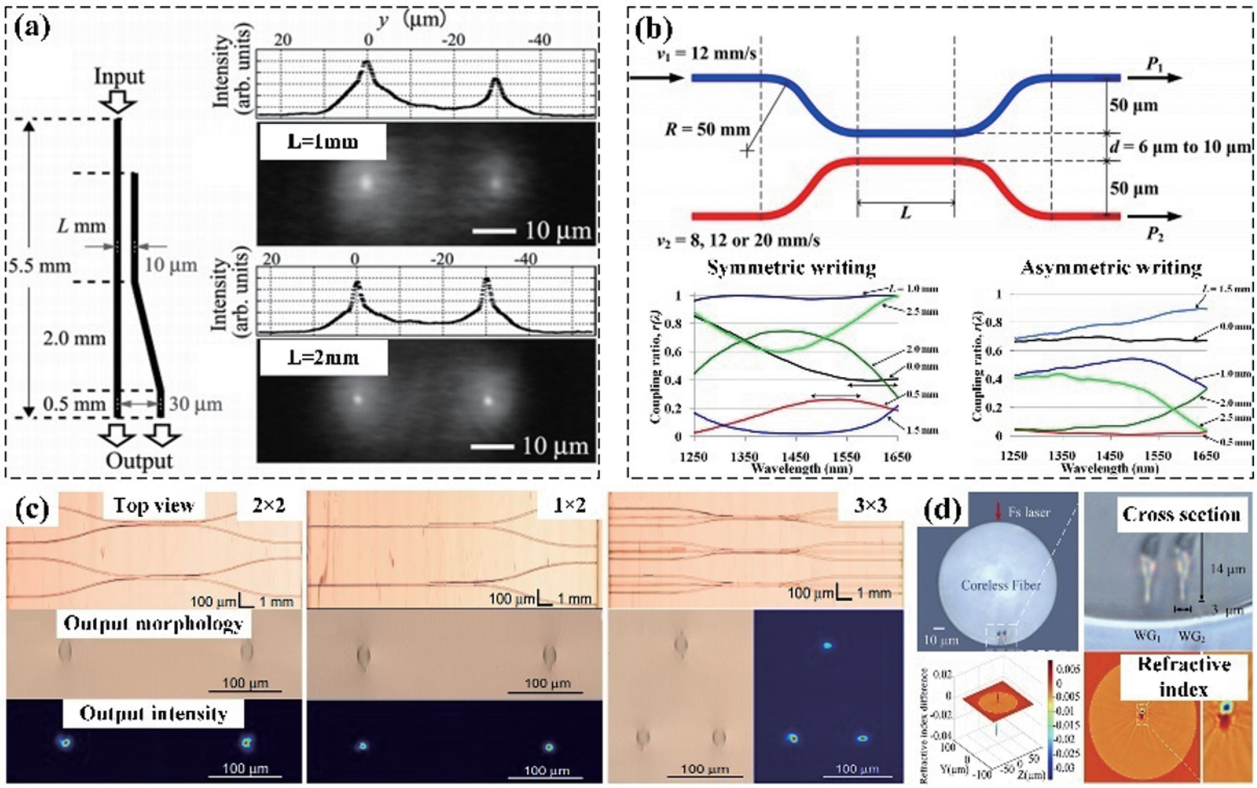

图 3　超快激光制备方向耦合器的部分研究成果。(a) PMMA 内的方向耦合器及不同耦合段长度下的分光比例[33]；(b)对称与非对称直写获得的方向耦合器在不同耦合长度、不同输入波段下的耦合效率[34]；(c)对称二向二分支、对称二分支和对称三向三分支型方向耦合器形貌和输出端能量分布[36]；(d)无芯光纤内的方向耦合器截面形貌及其周围材料的折射率分布[37-38]

Fig. 3　Several achievements of ultrafast laser manufacturing of directional couplers. (a) Directional coupler within PMMA and its splitting ratio under different coupling lengths[33]; (b) directional couplers obtained by symmetric and asymmetric writing and their coupling ratio under different coupling lengths and input laser wavelengths[34]; (c) morphology and intensity distribution at output face of symmetric 2×2, 1×2, and 3×3 directional coupler[36]; (d) cross-sectional morphology of directional coupler within coreless fiber and the refractive index distribution of surrounding medium[37-38]

耦合器的空腔直径均为 28 μm。Han 等[37]和 Zhang 等[38]在两根单模光纤之间拼接一段无芯光纤。在无芯光纤内利用超快激光直写出方向耦合器，两段波导间距为 6 μm，耦合段长度为 3 mm，如图 3(d)所示。该耦合器可用于探测周围介质的折射率变化，当折射率为 1.44～1.45 时，范围内分辨率可达 8249 nm/RIU，传输损耗为 1 dB/cm @ 1560 nm，耦合损耗约为 0.6 dB。

4.3　多模干涉光波导

多模干涉光波导型功率分配器一般由输入端、模混合区和输出端三部分构成。入射光从任意一个输入端入射，经过模混合区后，功率可以按照一定比例分配到所有输出端，光的模态亦会发生改变。

Watanabe 等[39]首次将直线光波导的末端与扁平状模混合区的中间连接，采用极低的直写速度(1 μm/s)在熔融石英内制出多模透射型干涉光波导，直线段直径为 2 μm，模混合区厚度为 2 μm。通过调整模混合区的长度和宽度，可以改变输出光的模态分布，如图 4(a)所示。Liu 等[40-41]设计了结构不同的多模透射型干涉波导，其长度为 870 μm，宽度为 2 μm，利用超快激光多道直写的方式在石英玻璃内制备出相应的波导结构，此举可有效扩大材料内的折射率变化范围(约为 2.5×10^{-3})。当脉冲能量从 0.43 μJ 增加至 0.53 μJ，波导的高度从 30 μm 提升到 48 μm，有效 NA 也从 0.25 降低至 0.2。波长为 632.8 nm 的单模激光从输入端进入波导后，高度为 30 μm 的多模干涉光波导输出 3 个波瓣，而高度为 48 μm 的多模干涉光波导输出 7 个波瓣，如图 4(b)所示。Chen 等[42]在单模光纤的纤芯中直写了具有负折射特性的平面光波导，并与未被直写的

区域一起构成了多模干涉光波导。透射测试结果表明，平面光波导段的长度越大，光信号的散射和衍射损耗越大，插入损耗也越高。当长度为 5 mm 时，该波导作为折射率探测器件时分辨率可达 10675.9 nm/RIU（折射率范围为 1.4484～1.4513），如图 4(c)所示。

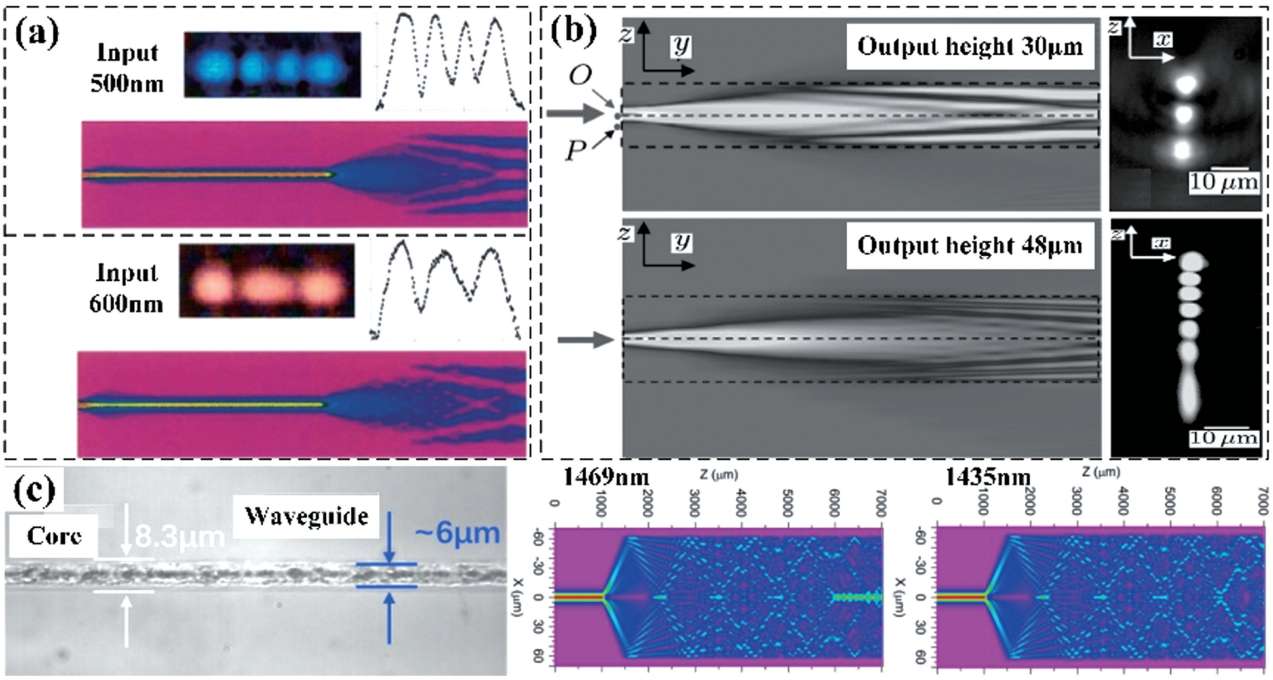

图 4　超快激光制备多模干涉光波导的部分研究成果。(a)多模干涉光波导的近场输出模态[39]；(b) 模混合区高度不同时多模干涉光波导的输出波瓣分布[40-41]；(c)作为折射率探测器的多模干涉光波导形貌及其工作时的光场分布[42]

Fig. 4　Several achievements of ultrafast laser manufacturing of multimode interference waveguides. (a) Near-field pattern at multimode interference waveguide output[39]; (b) lobe distribution at multimode interference waveguide output with different heights at mode mixing region[40-41]; (c) morphology and light field distribution of multimode interference waveguide when working as refractive detector[42]

5　波导型透镜的超快激光制备

波导型透镜是对在二维光波导内传输的导波光发挥透镜功能的器件，其与普通透镜类似，都具有成像和傅里叶变换功能。波导型透镜在成像中包含了会聚、发散和准直功能，在傅里叶变换中则包含了传递函数和信息代换，常见形式为膜折射率透镜、短程透镜、菲涅耳透镜和微透镜阵列等[43]。其中，超快激光在菲涅耳透镜和微透镜阵列制备中的应用较丰富。

5.1　菲涅耳透镜

菲涅耳透镜是利用光在周期性结构中的衍射现象制成的透镜，具有衍射、聚焦等功能。Watanabe 等[44]使用脉冲能量为 0.4 μJ 的超快激光在石英玻璃内烧蚀出空腔式透镜结构，这些空腔之间互相连接形成透镜。空腔边缘较为粗糙，导致实际衍射效率仅为 2%，如图 5(a)所示。Hasegawa 等[45]和 Srisungsitthisunti 等[46]则是利用液体晶体空间光调制器对准直的超快激光光束进行衍射，在石英玻璃内部直写出多路复用型菲涅耳透镜，通过调控激光的能量密度，可以改变透镜的直径和中心相位，进而改变透镜的有效数值孔径，结果如图 5(b)所示。Kim 等[47]采用超快激光直接烧蚀的方式，在无芯石英光纤端面刻蚀出菲涅耳透镜结构。根据近场电磁场分布的数值仿真结构，改变同心圆的直径以及刻蚀深度，在 632.8 nm 波段实现了透镜有效焦距的调控，如图 5(c)所示。Bricchi 等[48]将石英玻璃放置在微纳转台上，在工件表面 500 μm 以下的层面刻蚀出菲涅耳透镜结构。该透镜由 70 个同心圆环组成，最大的圆环半径为 1 mm，且圆环的凹结构和凸结构与上述研究[45-47]正好相反，即刻蚀的区域相反，如图 5(d)所示。聚焦实验结果表明，该透镜的衍射效率可达到 39%，接近理论极限值 40%[49]。Sun 等[50]利用轴锥镜将超快激光的能量分布调整为贝塞尔模式，在熔融石英内部直写出三层菲涅耳透镜结构，自上而下使用的直写速度逐层递减，形

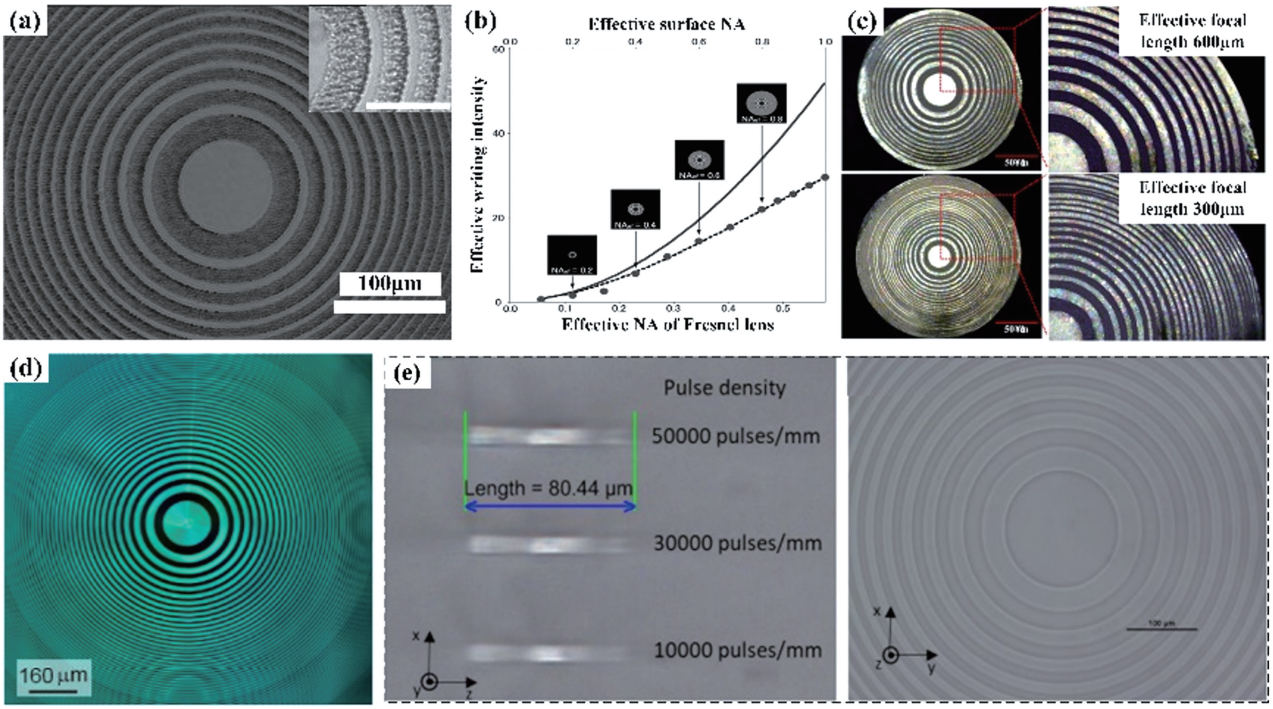

图 5　超快激光制备菲涅耳透镜的部分研究成果。(a)具有粗糙边缘和空腔内核的菲涅耳透镜形貌[44]；(b)有效直写能量密度与菲涅耳透镜有效数值孔径的关联[45-46]；(c)具有不同环数和直径的菲涅耳透镜形貌及其有效焦距[47]；(d)70 个同心圆环构成的菲涅耳透镜形貌[48]；(e)不同直写速度获得的多层菲涅耳透镜截面与表面形貌[50]

Fig. 5　Several achievements of ultrafast laser manufacturing of Fresnel lens. (a) Morphology of Fresnel lens with rough edge and void core[44]; (b) correlation between effective writing intensity and effective *NA* of Fresnel lens[45-46]; (c) morphology of Fresnel lens with different ring numbers and diameters as well as its effective focal length[47]; (d) morphology of Fresnel lens constructed by 70 concentric circles[48]; (e) cross-section and surface morphology of multi-layer Fresnel lens under different writing speeds[50]

貌如图 5(e)所示。相比于采用高斯分布的激光束，贝塞尔分布的激光直写效率可大幅提升。利用针孔法对其衍射效率进行表征，当针孔直径为 500 μm 时，衍射效率约为 52%。

5.2　微透镜阵列

微透镜是指直径在微米量级的微小透镜，由这些小透镜构成的阵列称为微透镜阵列。光波透过微透镜阵列时，波前受到同样的调制，经过衍射后继续传播，微透镜处光波的相位分布与输出平面上的光强是一一对应的。微透镜阵列主要应用于光源和探测器阵列中，可实现光束耦合、准直和会聚等功能，能够极大地提高耦合效率。

Cheng 等[51]和 Lin 等[52]采用四步法在光敏玻璃内制备微透镜阵列：超快激光以一定位移轨迹在工件表面刻划出微透镜阵列的基本轮廓；在 500～600 ℃的环境中进行热处理，然后随炉冷却，用以改变激光直写区域的晶相；将工件放置于质量分数为 10%的氢氟酸溶液中进行超声浴；在 560 ℃的环境中热烘，对透镜阵列表面进行平整化处理。获得的微透镜阵列及其聚焦后的光斑形貌如图 6(a)所示。Deng 等[53]则采用两步法在硅表面制备微透镜阵列。首先利用功率密度高达 1.25×10^{15} W/cm^2 的超快激光以高速直写的方式，在硅表面刻蚀出微坑结构；再将工件浸泡在质量比为 6∶10∶9 的氢氟酸、硝酸和乙酸混合溶液中超声浴，其中硝酸作为氧化剂，在硅表面形成氧化物，再由氢氟酸溶液将氧化物去除，将粗糙的凹坑修饰为光整的微透镜阵列，如图 6(b)所示。Cao 等[54]亦采用超快激光和化学刻蚀的方式在蓝宝石表面制备微透镜阵列。在超快激光直写光路中添加 4×4 全息点阵，直写效率可达 15.36 mm^2/min。直写后将工件放置于体积比为 1∶3 的磷酸和硫酸的混合液中，在 300 ℃的环境中热浴 90 min。处理后不同微透镜截面形貌的一致度可达 0.99944，具有高度的均一性，如图 6(c)所示。除圆形凸起和凹坑型的微透镜阵列外，Luo 等[55-57]利用轴锥镜将超快激光的能量分布调整为贝塞尔模式，分别在 PMMA、熔融石英表面直写出沟槽阵列。沟槽间的圆柱结构即构成了微透镜阵列，如图6(d)所示。相比于高斯分布激光

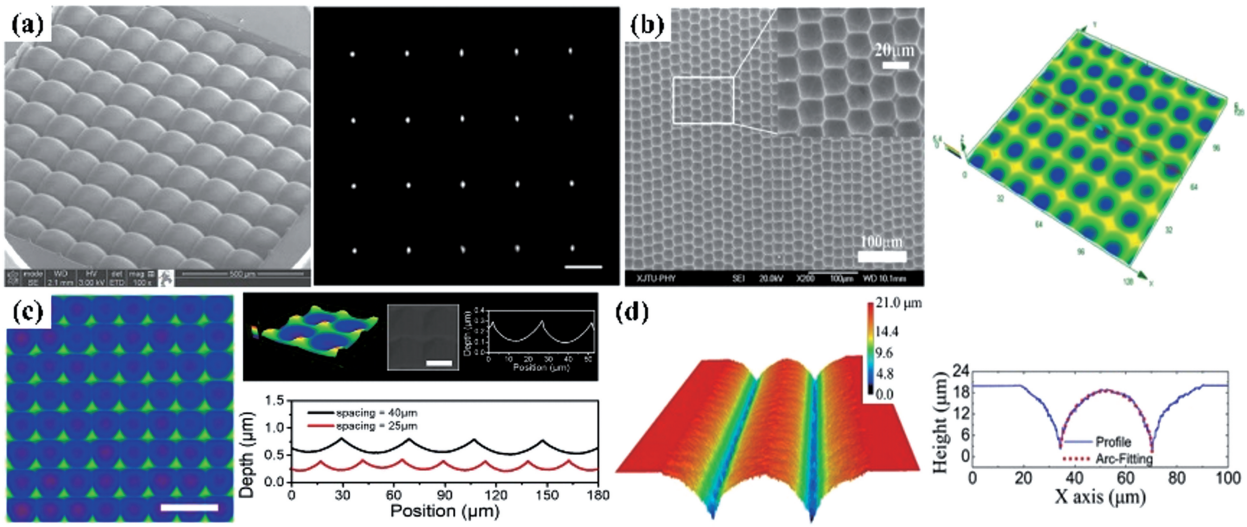

图 6　超快激光制备微透镜阵列的部分研究成果。(a)四步法制备的凸起状微透镜阵列及其聚焦后的光斑形貌[51-52]；(b)二步法制备的微坑状微透镜阵列[53]；(c)利用全息点阵直写的微透镜阵列[54]；(d)超快激光单步直写的圆柱状微透镜阵列[55-57]

Fig. 6　Several achievements of ultrafast laser manufacturing of microlens array. (a) Hump-like microlens array using a four-step fabrication technique and its focusing spot morphology[51-52]; (b) micro-crater-like microlens array using two-step fabrication technique[53]; (c) microlens array writed by holographic spot array[54]; (d) cylindrical microlens array fabricated by one-step ultrafast laser writing[55-57]

直写出的结构，该方法制备的微透镜阵列截面形貌更接近抛物线，对光束的聚焦效果更好。

综合以上分析，对超快激光在无源光波导器件制备中的代表性应用情况进行总结，如表 1 所示。

表 1　超快激光在无源光波导器件制备中的代表性应用

Table 1　Representative applications of ultrafast laser in the manufacture of passive optical waveguide devices

Waveguide device		Representative research team	Prominent achievement		
			Material	Technology	Device performance
Optical converter		Cheng Ya, from Shanghai Institute of Optics and Fine Mechanics, Chinese Academy of Sciences	Borosilicate glass[17]	Ultrafast laser writing and ultrasonic ethanol bath	Transmission loss 3–5 dB/cm@632.8 nm
			Fused silica[21-22]	Beam-shaped ultrafast laser writing, ultrasonic KOH etching and annealing	Transmission efficiency 90%@632.8 nm
Power splitter	Beam splitter	Chen Feng, from Shandong University	$LiNbO_3$[25]	Ultrafast laser writing	1×2 and 1×4 splitters, splitting angle 0.229°, transmission loss 3.4 dB/cm@632.8 nm
			$KTiOAsO_4$ crystal[30]	Ion implantation, ultrafast laser writing and annealing	1×2 splitter, minimum transmission loss 1.7 dB/cm@633 nm
	Directional coupler	Watanabe W, from Osaka University	PMMA[33]	Slit assisted ultrafast laser writing	Maximum refractive index change 4.6×10^{-4}, transmission loss 4.2 dB/cm@632.8 nm
		Li Yan, from Peking University	MgO-doped $LiNbO_3$[35]	Beam-shaped ultrafast laser writing	Maximum refractive index change 2.9×10^{-3}, transmission loss 2.58 dB/cm(H mode), 1.63 dB/cm (V mode)@1550 nm
	Multimode interference waveguide	Li Yan, from Peking University	Fused silica[41]	Ultrafast laser writing	Maximum refractive index change of 2.5×10^{-3}
		Shu Xuewen, from Huazhong University of Science and Technology	Single mode fiber[42]	Ultrafast laser writing	Refractive index 1.4484–1.4513, detection resolution 10675.9 nm/RIU

续表

Waveguide device		Representative research team	Prominent achievement		
			Material	Technology	Device performance
Waveguide lens	Fresnel lens	Kim J K, from Yonsei University	Mode-expanded hybrid opticalfiber[46]	Ultrafast laser ablation	Controllable effective focal length
		Gilberto B, from University of Southampton	Fused silica[49]	Ultrafast Bessel laser writing	Three layers structure, diffraction efficiency 52%
	Microlens array	Jiang Lan, from Beijing University of Technology	Photosensitive glass[51]	Slit assisted ultrafast laser ablation, thermal treatment, ultrasonic HF bath, thermal bake	Array area 150 μm×150 μm, effective diameter of focal spot 6–8 μm
		Duan Ji′an, from Central South University	Fused silica[55]	Beam-shaped ultrafast laser writing	Array area 5 mm×5 mm, effective *NA* higher than 0.35

6　总结与展望

自 20 世纪 90 年代以来，大量的理论与实验研究表明，超快激光可以在半导体、聚合物等材料内制备多种无源光波导器件。尤其在近些年，学者们在研究超快激光与多种波导材料作用机理的基础上，通过调制超快激光脉冲的时空分布等手段，在优化超快激光加工工艺的同时简化加工流程，实现了结构多样化、性能更为优异的无源光波导器件制备。为进一步提升制备无源光波导器件的质量和精度，仍需要从机理与工艺角度解决均质材料内部与异质材料界面热应力空间分布的定量分析与精准调控，针对多种材料实现突破衍射极限精度的可控加工等问题。

现阶段光电子集成器件向着多功能、高集成度的方向持续发展，这对作为集成器件的基本组成单元的无源光波导器件也提出了诸多挑战。一方面，其体积需要更加微型化，大规模生产时的效率需要进一步提高。另一方面，其应用不再局限于调整光信号的方向、功率配比以及能量分布等传统方向，而是与有源光波导器件集成，如激光器、调制器和探测器等，形成具有多功能、高性能的新一代光电子器件。此外，石墨烯等新兴材料也逐渐被引入无源光波导器件[58]。面向这些挑战，需要深入探索超快激光辐照下多种波导材料的光、热、电、力等物性的瞬态演变机制，在理论研究的指导下，开发超快激光纳米制造、高效并行制造技术，将超快激光在集成光学、量子信息和非线性光学等领域的应用进一步拓展。

参　考　文　献

[1] Min G. The situation of integrated circuit chip manufacturing in China[J]. Application of IC, 2019, 36(4): 24-28.
闵钢. 中国集成电路芯片制造业的状况分析[J]. 集成电路应用, 2019, 36(4): 24-28.

[2] Chollet F. Devices based on co-integrated MEMS actuators and optical waveguide: a review [J]. Micromachines, 2016, 7(2): 18.

[3] Halir R, Bock P J, Cheben P, et al. Waveguide sub-wavelength structures: a review of principles and applications[J]. Laser & Photonics Reviews, 2015, 9(1): 25-49.

[4] Zhang B, Li Z Q, Wang L, et al. Research advances in laser crystal optical waveguides fabricated by femtosecond laser direct writing [J]. Laser & Optoelectronics Progress, 2020, 57(11): 111415.
张彬, 李子琦, 王磊, 等. 飞秒激光直写激光晶体光波导的研究进展[J]. 激光与光电子学进展, 2020, 57(11): 111415.

[5] Mazur E. Femtosecond laser micromachining in transparent materials [C]//Bragg Gratings, Photosensitivity, and Poling in Glass Waveguides 2010, June 21-24, 2010, Karlsruhe Germany. Washington D.C.: OSA, 2010: BWB4.

[6] Dong M M, Lin G, Zhao Q Z, et al. Progress on femtosecond laser-fabricated waveguide devices in transparent dielectrics[J]. Laser & Optoelectronics Progress, 2013, 50(1): 010002.
董明明, 林耿, 赵全忠, 等. 飞秒激光在透明介质中制备波导器件进展[J]. 激光与光电子学进展, 2013, 50(1): 010002.

[7] Cai D K, Neyer A. Cost-effective waveguide

integration method for large-scale electrical-optical-circuit-board production [J]. Electronics Letters, 2010, 46(8): 581-583.

[8] Alden D, Guo W, Kirste R, et al. Fabrication and structural properties of AlN submicron periodic lateral polar structures and waveguides for UV-C applications[J]. Applied Physics Letters, 2016, 108(26): 261106.

[9] Ferrer A, de la Cruz A R, Puerto D, et al. *In situ* assessment and minimization of nonlinear propagation effects for femtosecond-laser waveguide writing in dielectrics [J]. Journal of the Optical Society of America B, 2010, 27(8): 1688-1692.

[10] Davis K M, Miura K, Sugimoto N, et al. Writing waveguides in glass with a femtosecond laser [J]. Optics Letters, 1996, 21(21): 1729-1731.

[11] Sundaram S K, Mazur E. Inducing and probing non-thermal transitions in semiconductors using femtosecond laser pulses [J]. Nature Materials, 2002, 1(4): 217-224.

[12] Stuart B C, Feit M D, Herman S, et al. Nanosecond-to-femtosecond laser-induced breakdown in dielectrics [J]. Physical Review B, 1996, 53(4): 1749-1761.

[13] Kanehira S, Si J H, Qiu J R, et al. Periodic nanovoid structures via femtosecond laser irradiation[J]. Nano Letters, 2005, 5(8): 1591-1595.

[14] Chan J W, Huser T, Risbud S, et al. Structural changes in fused silica after exposure to focused femtosecond laser pulses[J]. Optics Letters, 2001, 26(21): 1726-1728.

[15] Streltsov A M, Borrelli N F. Study of femtosecond-laser-written waveguides in glasses[J]. Journal of the Optical Society of America B, 2002, 19(10): 2496-2504.

[16] Chan J W, Huster T R, Risbud S H, et al. Waveguide fabrication in phosphate glasses using femtosecond laser pulses [J]. Applied Physics Letters, 2003, 82: 2371-2373.

[17] Sun H Y, He F, Zhou Z H, et al. Fabrication of microfluidic optical waveguides on glass chips with femtosecond laser pulses[J]. Optics Letters, 2007, 32(11): 1536-1538.

[18] Dreisow F, Heinrich M, Szameit A, et al. Spectral resolved dynamic localization in curved fs laser written waveguide arrays[J]. Optics Express, 2008, 16(5): 3474-3483.

[19] Arriola A, Gross S, Jovanovic N, et al. Low bend loss waveguides enable compact, efficient 3D photonic chips [J]. Optics Express, 2013, 21(3): 2978-2986.

[20] Lü J, Bai J, Zhou K M, et al. Transmission performance of 90°-bend optical waveguides fabricated in fused silica by femtosecond laser inscription [J]. Optics Letters, 2017, 42(17): 3470-3473.

[21] He F, Xu H, Cheng Y, et al. Fabrication of microfluidic channels with a circular cross section using spatiotemporally focused femtosecond laser pulses[J]. Optics Letters, 2010, 35(7): 1106-1108.

[22] He F, Lin J, Cheng Y, et al. Fabrication of hollow optical waveguides in fused silica by three-dimensional femtosecond laser micromachining [J]. Applied Physics B, 2011, 105(2): 379-384.

[23] Suzuki J, Arima Y, Yamaji M, et al. Curved-waveguide fabrication using femtosecond laser processing with glass hologram [J]. Proceedings of SPIE, 2010, 7589: 75890T.

[24] Liu Z M, Liao Y, Fang Z W, et al. Suppression of bend loss in writing of three-dimensional optical waveguides with femtosecond laser pulses [J]. Science China Physics, Mechanics & Astronomy, 2018, 61(7): 070322.

[25] Lü J, Cheng Y Z, Yuan W H, et al. Three-dimensional femtosecond laser fabrication of waveguide beam splitters in $LiNbO_3$ crystal [J]. Optical Materials Express, 2015, 5(6): 1274-1280.

[26] He R Y, Palmero I H, Romero C, et al. Three-dimensional dielectric crystalline waveguide beam splitters in mid-infrared band by direct femtosecond laser writing [J]. Optics Express, 2014, 22(25): 31293-31298.

[27] Ren Y Y, Zhang L M, Xing H G, et al. Cladding waveguide splitters fabricated by femtosecond laser inscription in Ti∶sapphire crystal [J]. Optics & Laser Technology, 2018, 103: 82-88.

[28] Cheng C, Romero C, de Aldana J R V, et al. Superficial waveguide splitters fabricated by femtosecond laser writing of $LiTaO_3$ crystal [J]. Optical Engineering, 2015, 54(6): 067113.

[29] Mittholiya K, Anshad P K, Mallik A K, et al. Inscription of waveguides and power splitters in borosilicate glass using ultrashort laser pulses [J]. Journal of Optics, 2017, 46(3): 304-310.

[30] Chen C, Akhmadaliev S, Romero C, et al. Ridge waveguides and Y-branch beam splitters in $KTiOAsO_4$ crystal by 15 MeV oxygen ion implantation and femtosecond laser ablation [J]. Journal of Lightwave Technology, 2017, 35(2): 225-229.

[31] Tao Q, Lu B W, Zhai Z S, et al. Manufacturing a 1×16 air-cladding polymeric optical splitter for electro-optical printed circuit boards by femtosecond laser [J]. Optical Engineering, 2020, 59(1): 017105.

[32] Landowski A, Zepp D, Wingerter S, et al. Direct

laser written polymer waveguides with out of plane couplers for optical chips[J]. APL Photonics, 2017, 2(10): 106102.

[33] Sowa S, Watanabe W, Tamaki T, et al. Symmetric waveguides inpoly(methyl methacrylate) fabricated by femtosecond laser pulses[J]. Optics Express, 2006, 14(1): 291-297.

[34] Chen W J, Eaton S M, Zhang H B, et al. Broadband directional couplers fabricated in bulk glass with high repetition rate femtosecond laser pulses[J]. Optics Express, 2008, 16(15): 11470-11480.

[35] Zhang Q, Li M, Xu J, et al. Reconfigurable directional coupler in lithiumniobate crystal fabricated by three-dimensional femtosecond laser focal field engineering[J]. Photonics Research, 2019, 7(5): 503-507.

[36] Skryabin N, Kalinkin A, Dyakonov I, et al. Femtosecond laser written depressed-cladding waveguide 2×2, 1×2 and 3×3 directional couplers in Tm^{3+}:YAG crystal[J]. Micromachines, 2019, 11(1): E1.

[37] Han J L, Zhang Y F, Liao C R, et al. Fiber-interface directional coupler inscribed by femtosecond laser for refractive index measurements[J]. Optics Express, 2020, 28(10): 14263-14270.

[38] Zhang Y F, Lin C P, Liao C R, et al. Femtosecond laser-inscribed fiber interface Mach-Zehnder interferometer for temperature-insensitive refractive index measurement[J]. Optics Letters, 2018, 43(18): 4421-4424.

[39] Watanabe W, Note Y, Itoh K, et al. Fabrication of multimode interference waveguides in glass by use of a femtosecond laser[J]. Optics Letters, 2005, 30(21): 2888-2890.

[40] Liu D, Li Y, An R, et al. Influence of focusing depth on the microfabrication of waveguides inside silica glass by femtosecond laser direct writing[J]. Applied Physics A, 2006, 84(3): 257-260.

[41] Liu D Y, Li Y, Dou Y P, et al. Transverse writing of multimode interference waveguides inside silica glass by femtosecond laser pulses[J]. Chinese Physics Letters, 2008, 25(7): 2500-2503.

[42] Chen P C, Shu X W, Shen F C, et al. Sensitive refractive index sensor based on an assembly-free fiber multi-mode interferometer fabricated by femtosecond laser[J]. Optics Express, 2017, 25(24): 29896-29905.

[43] Song G C, Quan W. Principle and devices of optical waveguide[M]. 2nd ed. Beijing: Tsinghua University Press, 2016: 67-72.
宋贵才, 全薇. 光波导原理与器件[M]. 2 版. 北京: 清华大学出版社, 2016: 67-72.

[44] Watanabe W, Kuroda D, Itoh K, et al. Fabrication of Fresnel zone plate embedded in silica glass by femtosecond laser pulses[J]. Optics Express, 2002, 10(19): 978-983.

[45] Hasegawa S, Hayasaki Y, Nishida N, et al. Holographic femtosecond laser processing with multiplexed phase Fresnel lenses[J]. Optics Letters, 2006, 31(11): 1705-1707.

[46] Srisungsitthisunti P, Ersoy O K, Xu X F, et al. Volume Fresnel zone plates fabricated by femtosecond laser direct writing[J]. Applied Physics Letters, 2007, 90(1): 011104.

[47] Kim J K, Kim J, Oh K, et al. Fabrication of micro Fresnel zone plate lens on a mode-expanded hybrid optical fiber using a femtosecond laser ablation system[J]. IEEE Photonics Technology Letters, 2009, 21(1): 21-23.

[48] Bricchi E, Mills J D, Kazansky P G, et al. Birefringent Fresnel zone plates in silica fabricated by femtosecond laser machining[J]. Optics Letters, 2002, 27(24): 2200-2202.

[49] Beresna M, Gecevičius M, Kazansky P G, et al. Polarization sensitive elements fabricated by femtosecond laser nanostructuring of glass[J]. Optical Materials Express, 2011, 1(4): 783-795.

[50] Sun Q, Lee T, Ding Z Q, et al. Diffractive Fresnel lens fabrication with femtosecond Bessel beam writing in silica[C]//Frontiers in Optics 2018, September 16-20, 2018, Washington, D.C., United States. Washington D.C.: OSA, 2018: JW3A.12.

[51] Cheng Y, Tsai H L, Sugioka K, et al. Fabrication of 3D microoptical lenses in photosensitive glass using femtosecond laser micromachining[J]. Applied Physics A, 2006, 85(1): 11-14.

[52] Lin C H, Jiang L, Chai Y H, et al. Fabrication of microlens arrays in photosensitive glass by femtosecond laser direct writing[J]. Applied Physics A, 2009, 97(4): 751-757.

[53] Deng Z F, Yang Q, Chen F, et al. Fabrication of large-area concave microlens array on silicon by femtosecond laser micromachining[J]. Optics Letters, 2015, 40(9): 1928-1931.

[54] Cao X W, Lu Y M, Fan H, et al. Wet-etching-assisted femtosecond laser holographic processing of a sapphire concavemicrolens array[J]. Applied Optics, 2018, 57(32): 9604-9608.

[55] Luo Z, Duan J A, Guo C L, et al. Femtosecond laser one-step direct-writing cylindrical microlens array on fused silica[J]. Optics Letters, 2017, 42(12): 2358-2361.

[56] Luo Z, Wang C, Yin K, et al. Rapid fabrication of cylindrical microlens array by shaped femtosecond laser direct writing[J]. Applied Physics A, 2016, 122(7): 1-5.

[57] Luo Z, Yin K, Dong X R, et al. Fabrication of parabolic cylindrical microlens array by shaped femtosecond laser[J]. Optical Materials, 2018, 78: 465-470.

[58] Ono M, Hata M, Tsunekawa M, et al. Ultrafast and energy-efficient all-optical switching with graphene-loaded deep-subwavelength plasmonic waveguides [J]. Nature Photonics, 2020, 14(1): 37-43.

Application of Ultrafast Lasers in the Manufacture of Passive Optical Waveguide Devices: A Review

Ding Ye, Li Qiang*, Li Jingyi, Wang Lianfu, Yang Lijun**

School of Mechatronics Engineering, Harbin Institute of Technology, Harbin, Heilongjiang 150001, *China*

Abstract

Significance With the development of aeronautics, astronautics, communication, and instrument fields, conventional optical and electrical systems can hardly meet the demand for information transmission with high capacity and rate. Integrated optics system gradually develops under this historical circumstance. Its superiority is that optical devices with different functions can be integrated into a limited area, and the optical signal can be transmitted and processed. Comparing with a conventional optical system, an integrated optics system has the superiorities of small size, compact structure, high stability, and strong anti-interference capability. The optical waveguide device is the most basic unit within the integrated optics system. Its principle is that total reflection takes place at the media interface when light transmits in media with different refractive indexes, and light can be trapped in the microstructures. A channel forms correspondingly, in which light is capable of transmitting along a specific direction. Optical waveguide devices can trap and guide light and provide extra functions such as nonlinearity and active gain. Besides, optical waveguide devices can cooperate with other components in the integrated optics system, forming a photonic integrated circuit with various functions. Therefore, the performance of the optical waveguide device has a considerable influence on the performance of an integrated optics system. The development of manufacturing technology for optical waveguide devices with high quality and precision of great importance for the innovation of photocommunication, optical information processing, optical calculation, and optical sensing.

Optical waveguide devices can be divided into passive and active devices. The former devices are the basic units of integrated optoelectronics, and they are more widely used. Passive waveguides are mainly fabricated using semiconductors and organic polymers. There are three types of semiconductor waveguides, listed as silicon-based waveguides, III-IV group compounds waveguides, and ferroelectric oxides waveguides. Specifically, silicon-based waveguides have the advantages of good heat conductivity, chemical stability, mechanical strength, and low absorption loss. However, there is a large difference between the refractive indexes of cladding and core. The advantage of III-IV group compounds waveguides is that they can be integrated on the same chip with active devices. However, the large transmission loss and cost limit their further application. The advantages of ferroelectric oxides waveguides are large electrooptic coefficient, high response speed, and excellent heat and chemical stability. However, they are still troubled by high cost and large size. In terms of organic polymer waveguides, they are characterized by low optical loss and birefringence, high thermooptical and electrooptical coefficients as well as simple fabrication techniques. Unfortunately, they age easily, which is unfavorable for improving the device stability.

In 1996, Davis K M manufactured an optical waveguide with optical glass for the first time. In the following decades, with the development of ultrafast laser systems and optimization of manufacturing technology, researchers from home and abroad have successfully manufactured various optical waveguides in different materials. Although several remarkable advances have been made in improving device performance, the industrial fields are still troubled with several problems, such as non-negligible machining defects and transmission loss. Hence, it is of great significance to summarize the existing research to guide the future development of manufacturing technology for passive waveguide devices.

Progress The interaction mechanism between laser and waveguide materials is first explained. On these bases, the application of ultrafast laser in the manufacture of optical path converter is firstly interpreted. As a common optical path converter, the morphologies of curved waveguides before or during the performance test are shown (Fig. 1). Then, the morphologies and performances of three kinds of power splitters, listed as a branched waveguide (Fig. 2), directional coupler (Fig. 3), and multimode interference waveguide (Fig. 4), fabricated using ultrafast laser and other auxiliary means are illustrated. The waveguide lens can be divided into Fresnel lens and microlens array, the corresponding morphologies fabricated by ultrafast laser are demonstrated as well (Figs. 5–6). At last, the representative applications of ultrafast laser in the manufacture of passive optical waveguide devices are summarized (Table 1), in which the leading research teams and their achievements are highlighted.

Conclusions and Prospect Since the 1990s, a large number of theoretical and experimental studies have pointed out that ultrafast lasers are effective tools to fabricate various passive optical waveguides in dielectrics and polymers. Especially in recent years, based on the investigation of the interaction mechanism between ultrafast lasers and different waveguide materials, researchers have achieved the fabrication of passive waveguides with multiple structures and excellent performance by adjusting the temporal and spatial distribution of laser pulses. The fabrication techniques are optimized, and the process is simplified. To further improve the fabrication quality and precision, there are still several existing problems that need to be solved from the aspects of mechanism and techniques. For instance, the quantitative analysis and precise modulation of the spatial distribution of thermal stress induced by ultrafast lasers within the same material as well as the interface between different materials and the controllable fabrication of different materials with a precision that exceeds the diffraction limit.

Nowadays, integrated optoelectronic devices are developing toward multifunctions and high integrated levels, which raises great challenges for passive optical waveguides. On the one side, their volumes need to be minimized, and production efficiency needs to be improved further. On the other side, their applications are not only limited to treating light signals, but also integrated with active optical waveguides, such as lasers, modulators, and detectors to construct new-generation optoelectronic devices. Besides, novel materials such as graphene have been used to fabricate passive waveguides. To deal with these challenges, the transient evolution mechanisms of light, heat, electrical, and mechanical properties of different waveguide materials irradiated by ultrafast lasers should be investigated deeply. Under the guidance of theoretical studies, nanofabrication and parallel fabrication technologies can be developed that are beneficial for extending the application of ultrafast lasers in modern industrial fields, such as integrated optics, quantum information, and nonlinear optics.

Key words laser technique; ultrafast laser; passive optical waveguide device; manufacturing technology; device performance

OCIS codes 140.7090; 230.7370; 120.4610